This is the author's accepted version of the article. The final version published by IEEE is S. Mishra, A.F. Zanella, O.E. Martínez-Durive, D. Madariaga, C. Ziemlicki and M. Fiore, "Characterizing 5G Adoption and its Impact on Network Traffic and Mobile Service Consumption," IEEE INFOCOM 2024 - IEEE Conference on Computer Communications, 2024, pp. TBD, doi: TBD

Characterizing 5G Adoption and its Impact on Network Traffic and Mobile Service Consumption

Sachit Mishra*†, André F. Zanella*†, Orlando E. Martínez-Durive*†,
Diego Madariaga*, Cezary Ziemlicki‡, Marco Fiore*
*IMDEA Networks Institute, Spain, †Universidad Carlos III de Madrid, Spain, ‡SENSE / Orange Innovation, France
{sachit.mishra, andre.zanella, orlando.martinez, diego.madariaga, marco.fiore}@imdea.org, cezary.ziemlicki@orange.com

***Abstract*—The roll out of 5G, coupled with the traffic monitoring capabilities of modern industry-grade networks, offers an unprecedented opportunity to closely observe the impact that the introduction of a new major wireless technology has on the end users. In this paper, we seize such a unique chance, and carry out a first-of-its-kind in-depth analysis of 5G adoption along spatial, temporal and service dimensions. Leveraging massive measurement data about application-level demands collected in a nationwide 4G/5G network, we characterize the impact of the new technology on when, where and how mobile subscribers consume 5G traffic both in aggregate and for individual types of services. This lets us unveil the overall incidence of 5G in the total mobile network traffic, its spatial and temporal fluctuations, its effect on the way 5G services are consumed, the way individual services and geographical locations contribute to fluctuations in the 5G demand, as well as surprising connections between socioeconomic status of local populations and the way the 5G technology is presently consumed.**

I. Introduction

As the deployment of 5G networks is advancing globally, understanding the evolution, performance, and impact on users of this new generation of cellular technology is critical. However, due to industrial secrecy and competition in an aggressive market, operators tend to publicly disclose minimum information about their planning strategies for 5G or about the impact that the technology has on their users.

Market analyses by a leading actor like Ericsson [1] indicate that the adoption of 5G is well en route, with a declared coverage of the world population that has reached 35%. In Western Europe, which will be the focus of our study, that figure was already at 79% at the end of 2022. The improving coverage is in turn uplifting the adoption of the technology by users. As a matter of fact, the total number of 5G subscriptions is projected to reach the 1.5 billion mark in 2023, with a growth of 500 million within the last 12 months, and a twofold increase in the past two years. In Western Europe, 5G subscribers rose from 32 million in 2021 to 69 million at the end of 2022, and there are general expectations that 4G will start to decline in favor of 5G from 2023 onward. This leads to forecasts that 5G shall attain 143 million subscribers in the region by the end of 2023, and a 88% penetration by the end of 2028, also leading to the dismissal of 3G radio access to enable spectrum reuse for 5G.

While these figures are interesting, they only provide a high-level picture of the adoption of the 5G technology. Many interesting questions related to if and how the availability of a higher-performance wireless technology is affecting the way subscribers consume mobile traffic and services remain unanswered. For instance, we have little clarity on: how the 5G technology is employed by users over space and time, and whether such patterns differ from those observed for 4G; if 5G is changing the utilization of specific mobile applications; or, whether there are specific portions of the population that are adopting the technology faster than others. In this paper, we provide a very first in-depth analysis into the utilization of 5G by the whole user population of a major mobile network operator. Building on three months of data collected between March and May 2023 in a production network serving France, we bring forth a new understanding on the impact of 5G on the spatial and temporal dynamics of both total traffic and service-level demands. Among our key insights, we highlight:

- the adoption of 5G is still at relatively early stages in France with a low growth rate and a consumption that is very strongly oriented at the main urban areas, although with large discrepancies within cities;
- the availability of high-speed 5G connectivity affects services and devices (*e.g.*, iOS versus Android) in very diverse ways, and pushes users to consume applications much more intensively, seemingly towards closing the gap with typical usages of fixed Internet access;
- the fraction of overall mobile traffic contributed by 5G is surprisingly not constant in time, rather it shows a clear circadian rhythm with strong overnight peaks, which are in fact generated by a subset of download-intensive applications consumed in specific urban neighborhoods;
- the regions generating the aforementioned peak and higher 5G incidence in general are in fact characterized by lower education and income, suggesting that the local population makes a significant use of 5G 'dongles' as a replacement for the more expensive fiber Internet access.

II. Related work

A handful of previous studies have investigated the deployment and performance of the 5G technology, typically in deployments located in the United States or in China. Almost all such prior works build upon client-side measurements, and target the evaluation of coverage, latency, energy consumption, or protocol operations observed at the level of individual 5G devices, usually providing results that employ 4G as a reference. Several of these measurement analyses target specific scenarios, such as Non-Standalone (NSA) and Standalone (SA) deployments [2], mmWave communications [3], multiple

operators [4], [5], diverse urban environments [4], bus transit system [6], or high-speed trains [7].

These works generally acknowledge the much improved throughput of 5G compared to 4G, yet also highlight a number of issues, including sub-optimal latency and high power consumption with respect to 4G [8], exceedingly aggressive strategies for the migration of radio resources from 4G to 5G [9], non-ideal support for high mobility scenarios [7], or inadequate resource management policies [5]. Some works also propose solutions to some of the problems above [5] or optimizations of applications to best utilize 5G features [2].

Unlike all client-side studies above, in this paper we take a network perspective, analyzing traffic measurements collected by a major mobile operator in a nationwide production-grade infrastructure. This offers a completely different viewpoint, and allows in particular for an analysis of the spatiotemporal demands generated by the whole user population, which is very hard to obtain from smartphone measurements.

To the best of our knowledge, there is a single paper that performed a large-scale network-side investigation of 5G before, by Parastar *et al.*, [10]. The authors studied an operational 5G NSA network in the UK, and focused on understanding the temporal evolution and characteristics of the local deployment, the diversity on the ecosystem of 5G-enabled devices, and the overall network performance. Our paper has a very different aim, as it primarily targets the characterization of 5G adoption over space and time, with a strong emphasis on the consumption of individual services. Neither spatiotemporal nor application-level aspects were instead considered by Parastar and colleagues.

A number of previous works investigated mobile services demands and their dynamics over space and time. Examples include analyses of single applications like WhatsApp [11] and WeChat [12], broad service categories such as video streaming [13] and Cloud services [14], or ample ranges of diverse applications [15], [16], [17]. Earlier research unveiled a number of properties of service-level demands, such as the fact that they exhibit locality [18], [19], [20], temporal patterns that are diverse across applications [16] and possibly easy to predict [21], as well as consistent user bases [22], [23]. However, all these works employ demands collected in 3G or 4G networks, and do not look into adoption of one technology over another. Ours is the very first study to inquire into the impact of a new mobile technology on application usage.

III. Data measurement and processing

Our study builds upon measurement data collected in a nationwide mobile network providing coverage in France. We next present the data collection platform, the data preprocessing routines, and how the whole pipeline abides by ethical research principles.

A. Data collection platform

The monitored network infrastructure offers 2G, 3G, 4G, and 5G non-standalone (NSA) radio access technologies (RATs). We recall that NSA has 5G gNodeBs coexist with 4G eNodeBs in the radio access network (RAN), so as to provide higher-capacity wireless communication to 5G-capable UEs. Yet, the lack of a dedicated 5G network core in the NSA deployment forces gNodeBs to depend on interactions with eNodeBs, via the X2 interface, for control operations towards the 4G Mobility Management Entity (MME). Also, gNodeBs connect to Serving Gateways (SGWs) and Packet Gateways (PGWs) of the 4G Evolved Packet Core (EPC) via a slightly modified S1-U interface for all data plane transmissions.

We employed production-grade passive probes deployed at PGWs, which serve both 4G and 5G users, to gather data about the vast majority[1] of individual transport-layer sessions established within the entire network infrastructure during 92 consecutive days, from March 1 to May 31, 2023. The PGW probes ran proprietary traffic classifiers developed by the operator and based on Deep Packet Inspection (DPI) to identify the mobile service generating each session[2]. Every session was associated to the carriers (*i.e.*, antennas) serving it over time using signaling data from the MME, which again manages both 4G and 5G control planes. This allowed to accurately georeference (portions of) each session to the location of cellular sites where the serving carriers are deployed.

Individual session data was then processed within the secure computing premises of the network operator, so as to produce hourly aggregates of the overall traffic demand generated by every mobile service at each of the $266,368$ carriers of the 4G and 5G RATs present in the monitored RAN.

B. Areal interpolation to statistical zones and filtering

We perform an aerial interpolation of the carrier-level traffic data onto $48,949$ statistical zones (also referred to simply as 'zones' in the following) defined by the pertinent national institute for statistics, which eases spatial filtering and downstream analyses of the data performed throughout our study. To this end, we adopt a common strategy of computing a Voronoi tessellation [24] of space on the locations of RAN sites, and uniformly spreading the traffic associated to each carrier over the surface of the Voronoi cell associated to its site. Then, each zone is assigned the traffic demand lying within its surface.

Examples of this procedure are illustrated in Figure 1b and 1c for two statistical zones. These figures in fact illustrate how different zones can experience very diverse 5G coverage quality: the zone in Figure 1b is largely covered by sites equipped with 4G carriers only, whereas that in Figure 1c is almost completely covered by sites where both 4G and 5G carriers are present. Figure 1a offers a quantitative perspective on this diversity, reporting the number of statistical zones having a given percentage of their surface covered by 5G-enabled sites. The histogram is clearly dominated (note the logarithmic scale of the ordinate) by the peaks around 0%

[1] According to separate measurements, 2G and 3G accounted for less than 0.5% of the data traffic in the region under study during the first quarter of 2023. Our analysis thus focuses on the largely dominant 4G and 5G RATs.

[2] Overall, the 100 mobile services generating the most traffic are monitored, which include popular applications like Instagram, Netflix, YouTube, Twitter, Skype, Spotify, Pokemon Go, and iCloud, just to cite a few. These services are responsible for 63% of the total 4G and 5G traffic in the network.

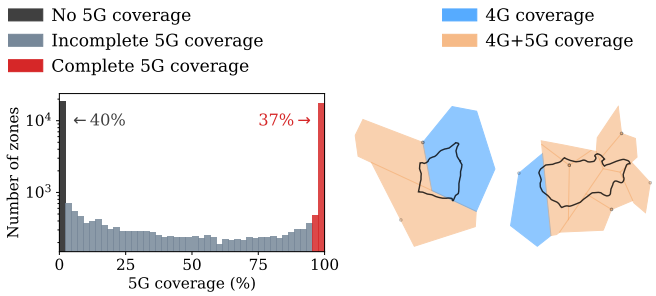

(a) (b) (c)

Fig. 1: (a) 5G coverage across statistical zones. Samples of zones mainly covered by (b) 4G only and (c) 4G and 5G.

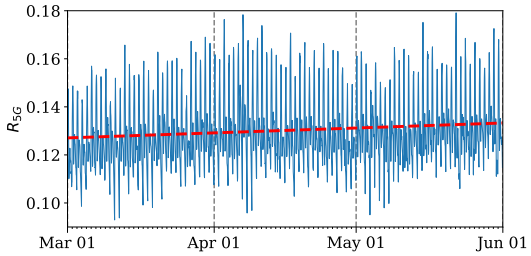

Fig. 2: Nationwide 5G ratio, computed on an hourly basis during the three-month observation period. Linear trend in red.

and 100%, indicating that zones tend to be well covered or not covered at all. It also highlights how 5G coverage is still far from pervasive in France, with 36% of zones having a 5G coverage above 95% (denoted in red in the figure).

In the rest of our study, we will precisely focus on those L=18,014 statistical zones that have a complete 5G coverage. The rationale is that such zones offer a 5G coverage quality that is comparable to that provided by 4G, and enable a fair comparison between the two RATs. An analysis of the RAN configuration in the selected zones confirms that (i) a high fraction of 78% of the cellular sites located within their boundaries are 5G enabled, and (ii) 5G carriers have identical azimuths to those of local 4G carriers in those sites, which further point at a roughly equivalent 4G and 5G coverage.

C. Ethics considerations

The traffic measurements used to derive the aggregate service demands were collected by the operator for network management and research purposes, and temporarily stored within a secure platform at their own premises. The raw data processing was also carried out in the same platform by personnel of the network operator, in full compliance with Article 89 of the General Data Protection Regulation (GDPR) [25] of the European Commission. The data collection and processing were approved by the Data Protection Officer (DPO) of the operator, and authorized by the relevant national privacy-protection agency.

The researchers involved in our study only had access to such aggregates, whose spatiotemporal resolution ensures that no data subject can be re-identified from the data, which in fact does not configure as personal data in the GDPR acceptation.

IV. Overview of Nationwide 5G Adoption

We start by providing a high-level analysis of 5G adoption in France, exploring what fraction of traffic 5G users currently generate, and how it varies in space and time.

A. How much traffic does 5G generate?

In order to quantify the incidence of 5G on the mobile data usage, we will employ throughout the paper the notion of *5G ratio*, *i.e.*, the fraction of broadband traffic generated via the 5G technology. Formally, the 5G ratio measured at a given statistical zone ℓ and over a time period t is defined as

$$R^{\ell}_{5G}(t) = \frac{v^{\ell}_{5G}(t)}{v^{\ell}_{4G}(t) + v^{\ell}_{5G}(t)}, \quad (1)$$

where $v^{\ell}_{\star}(t)$ is the volume of data traffic generated by technology $\star$. Based on (1), $R^{\ell}_{5G}(t) = 0$ if 5G demands are absent and the mobile traffic is only generated by 4G devices, whereas $R^{\ell}_{5G}(t) = 1$ if 5G has already seized the whole user demand.

Figure 2 shows the evolution of the nationwide 5G ratio $R_{5G}(t) = 1/L \cdot \sum_{\ell} R^{\ell}_{5G}(t)$, at hourly time steps t and over the full data collection period. We observe that $R_{5G}(t)$ ranges typically between 0.10 and 0.18, *i.e.*, 5G users are responsible for 10% to 18% of the overall mobile data traffic served by the operator across France. The average value recorded over the three-month period is 0.1302, which can be used as a high-level figure for the penetration of 5G demands: in other words, in geographical regions where 5G service is available and well provisioned, 5G users typically generate 13% of the total mobile data traffic.

Interestingly, the average nationwide 5G adoption is not constant in time: it increases from 12.7% on March 1 to 13.3% on May 31. The dashed red line in Figure 2 reports the result of a linear fit on the data, which displays a clearly positive slope. Therefore, the incidence of 5G demands is steadily growing within areas where the new RAT is present, exposing how 5G is gaining momentum. While the trend is expected, from the fitting we can quantify the effect and estimate a mean increment of 0.05 percent points per week at a national scale.

Key insights. *In areas of France where the 5G technology is pervasive, the 5G demand accounts for around 13% of the overall mobile broadband traffic. According to projections from our observation period, that percentage is growing at a pace of 2.4 points per year. These figures indicate that the adoption of 5G is still at early stages in France, and is relatively slow in gaining 4G market shares.*

B. How is 5G traffic consumed over time?

Figure 2 shows that the 5G ratio of traffic aggregated over the whole country, $R_{5G}(t)$, undergoes substantial fluctuations between different hours, which prompts a deeper investigation of temporal patterns in 5G adoption. To this end, we look at *median weeks*, *i.e.*, one-week time series that summarize in a compact way the typical fluctuations of the target temporal

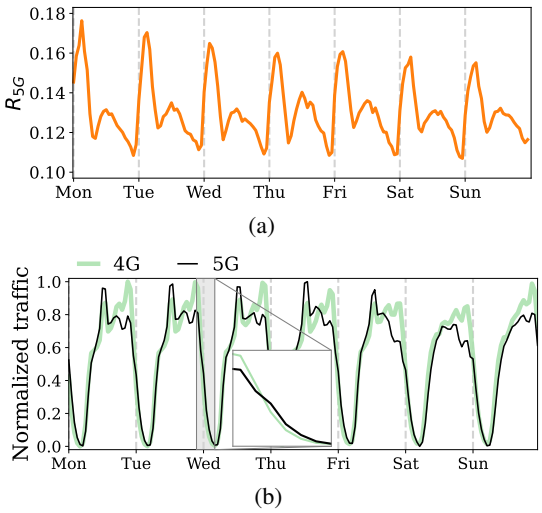

Fig. 3: (a) Median week of 5G ratio in total traffic. (b) Median weeks of the traffic demands separated by technology.

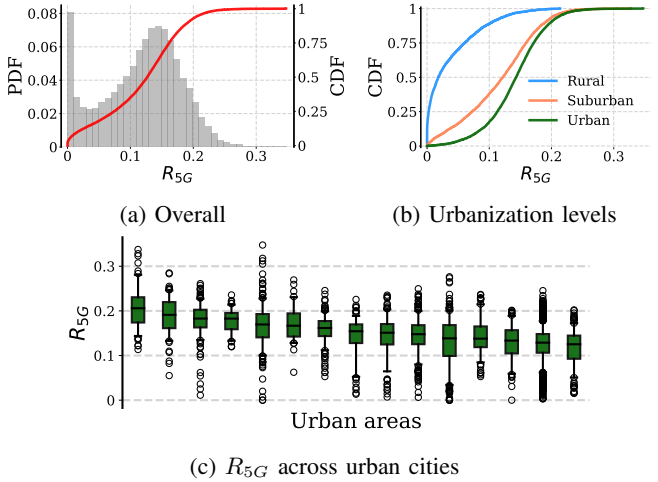

Fig. 4: (a) CDF of the overall 5G ratios over the total traffic across zones. (b) Breakdown of CDFs across urbanization levels. (c) Distribution of the ratio of 5G traffic across multiple cities. Boxes represent the range between the first and third quartiles, and encase the median line. Whiskers represent the 5$^{\text{th}}$ and 95$^{\text{th}}$ percentiles, and fliers are outside this range.

phenomena, as the median value of each hour of the week across all weeks in the dataset. Figure 3a depicts the median week of $R_{5G}(t)$, and unveils a very clear daily periodicity: the fraction of mobile data traffic contributed by 5G in the whole country has (i) a high peak overnight, between 22:00 and 7:00 (8:00 during weekends), (ii) a smaller second peak in the first part of the day, and (iii) a drop in the afternoon until 22:00.

To ease the interpretation of the result, Figure 3b shows min-max normalized time series of the median weeks of nationwide 4G and 5G traffic. We recall that these time series refer to statistical zones where both technologies are pervasive, as per Section III-B, hence can be fairly compared. We observe that 4G and 5G traffic exhibit notably different time patterns. First, dynamics are similar throughout the morning, which results in $R_{5G}(t) \sim 0.13$ in Figure 3a during that period: that is, 4G and 5G users behave in a similar way in the first part of the day, and the 5G ratio is fairly stable around its typical value recorded in Section IV-A. Second, patterns diverge in the afternoon, as 5G demands drop while 4G traffic grows, which explains the decrease in $R_{5G}(t)$ in the second part of the day. Third, as seen in the inset plot, the trend switches from 22:00 through the night, as the 5G traffic curve has a less steep slope which leads to higher (relative) values overnight: this leads to the $R_{5G}(t)$ peaks that last until early in the morning.

Key insights. *The incidence of 5G is not uniform over time, rather it follows a neat circadian pattern with fluctuations that make the 5G incidence almost double within each single day. The reason is that, quite surprisingly, 4G and 5G demands do not follow the same temporal dynamics through the day. We will investigate the reasons of this phenomenon in Section VI.*

C. Where is 5G traffic consumed?

All results presented before are aggregated over the whole country, yet 5G adoption is not necessarily heterogeneous over the territory. Figure 4a shows the Probability Density Function (PDF) and Cumulative Distribution Function (CDF) of the mean 5G ratio computed at statistical zones ℓ, *i.e.*, $R^{\ell}_{5G} = 1/T \cdot \sum_t R^{\ell}_{5G}(t)$, where T is the number of hourly time steps t in our dataset. The distributions show how different zones experience very different 5G traffic incidence, ranging all the way from zero in some zones up to 35% in others. In particular, the PDF spotlights a clear peak of almost 10% of zones without 5G users. We recall that all zones considered enjoy pervasive 5G coverage, hence RAT availability cannot be the root cause of the diverse adoption.

A great portion of the spatial diversity, including the peak at R^{ℓ}_{5G}=0, is in fact ascribed to the urbanization level of the region where the zone is located. Figure 4b breaks down the R^{ℓ}_{5G} CDF across urban, suburban and rural areas that are covered by 5G, and exposes how lower incidence almost exclusively emerges in rural 5G deployments, where half of the zones experience less than 5% 5G traffic; by contrast, no statistical zone in urban areas has such a low 5G adoption. Similarly, the percentage of zones where 5G users generate more than 10% of total traffic, *i.e.*, R^{ℓ}_{5G}>0.1, is just 10% in rural regions but jumps to more than 80% of urban environments.

In light of these observations, we focus the analysis on major conurbations, and consider the 15 largest metropolitan areas in France, which jointly include 35% of the urban and suburban zones where 5G incidence is significant as per Figure 4b. The 5G ratios R^{ℓ}_{5G} recorded in all statistical zones of one city are summarized into a single candlestick in Figure 4c: by juxtaposing the summaries of different cities, we observe fairly comparable 5G ratios, with medians that indicate a typical 5G adoption well above 10% in all cases, vary by 0.05 at most, and have a similar span of percentiles.

In fact, Figure 4c reveals how the spatial heterogeneity of 5G adoption is much larger *within* cities than *across* them: the intervals between the 5$^{\text{th}}$ and 95$^{\text{th}}$ percentiles tend to traverse 15 to 30 percent points in the 5G adoption across zones within

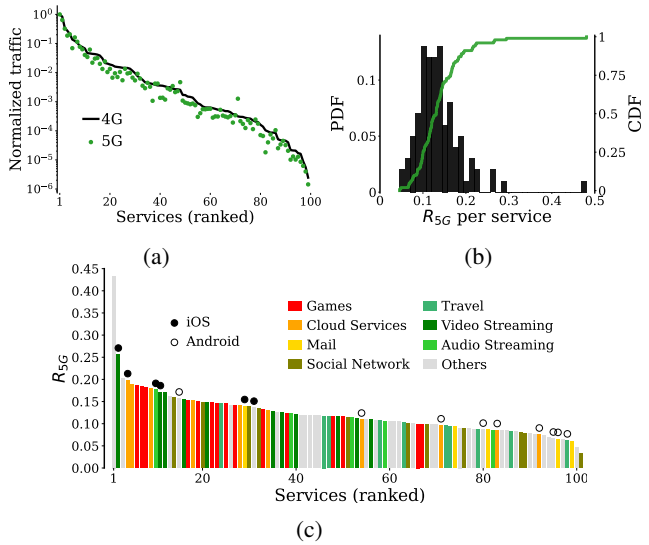

Fig. 5: (a) Ranking for the top 100 services by their total traffic volume, for 4G and 5G, with values normalized per technology. (b) PDF and CDF of the 5G ratio across services. (c) Ranking of mobile applications based on their 5G ratio.

a same city. In other words, almost all the variety observed in the CDFs in Figure 4b can be found within each single city.

Key insights. *5G adoption remains a prominently urban phenomenon to date in France, with all major cities experiencing similar levels of incidence of 5G demands on the total traffic. Yet, 5G usage becomes highly diverse among neighborhoods of each conurbation. We will investigate these intra-city spatial diversities in detail in Section VI.*

V. A SERVICE-LEVEL PERSPECTIVE ON 5G ADOPTION

The introduction of a new RAT is a unique opportunity to explore if users of specific mobile services are taking particular advantage of the more performing communication technology. In this section, we study how 5G adoption breaks down across individual mobile services, and how it affects their behavior.

A. Is 5G adoption uniform across mobile services?

First, we look at whether the introduction of 5G has impacted the popularity of services among users. Figure 5a shows a ranking of the first 100 mobile services, based on the their 4G traffic volume (black line), with associated 5G volumes (green dots). Both 4G and 5G service-level traffic volumes are normalized by the demand of the first service in each technology. The quasi-linear curve over the logarithmic ordinate confirms the well-known power-law behavior of service-level demands [26], [16], which are highly skewed and encompass six orders of magnitude within the first 100 applications. More interestingly, the 5G traffic dots are mostly well aligned along the 4G curve, indicating that 5G does not bring any substantial change in the popularity ranking of services.

More interesting patterns emerge when considering the 5G ratio at a per services level. Figure 5b shows the PDF and CDF of the nationwide time-averaged 5G ratio, *i.e.*, $R_{5G} = 1/(LT) \cdot \sum_\ell \sum_t R^\ell_{5G}(t)$, computed for each individual mobile service. The distributions show that the incidence of 5G is very heterogeneous across applications: the Gaussian-shaped PDF has an average around R_{5G}=0.13 that reflects the overall 5G ratio discussed in Section IV-A, but then spans all the way from services that have less than 5% 5G traffic to others than have almost 50% of their demand served by 5G already.

Figure 5c offers a more in-depth view on such a diversity, as a ranking of applications based on their R_{5G} value. Services are also associated to specific classes (*i.e.*, colors), and those that are highly platform-specific (*e.g.*, Apple Music for iOS, or Google Play Store for Android) are tagged with filled (iOS) or empty (Android) markers. We note loose patterns at the level of service classes, such as gaming, video streaming, and Cloud services having a tendency to display higher 5G ratios, yet no strong conclusion. A more clear correlation emerges between R_{5G} and device types: iOS-specific applications consistently appear at the top of the ranking (with an average R_{5G}=0.18), while Android-based ones are gathered at the bottom (with an average R_{5G}=0.09). This suggests that Apple users are well ahead of the 5G adoption curve, which aligns well with the fact that they tend to be early technology adopters [27].

Key insights. *While the popularity of mobile services is not impacted by the introduction of 5G, individual services do show very a diverse incidence of 5G in their demands. This diversity is not strongly linked to the type of application, but our analysis suggests that the penetration of 5G among Apple users is around twice that observed in non-Apple users.*

B. Does 5G affects the way services are consumed?

The 5G ratio analysis above relies on traffic demands, hence looking at the impact of 5G on popular applications in terms of sheer *usage volume*. A different and interesting question is if 5G is also changing the *way* each such service is consumed.

The uplink-to-downlink (UL/DL) traffic ratio captures the imbalance between traffic from and to the mobile device, and is a good indicator of the high-level behavior of the utilization that subscribers make of a given mobile application [16]. Figure 6a portrays CDFs of the UL/DL ratio across the top 100 services, separately for traffic accommodated by 4G and 5G RATs. The overall CDFs appear relatively close between the two technologies, yet substantial differences emerge when taking a closer look, in the inset plots. In particular, the CDFs cross each other, meaning that 5G entails a higher probability of very low UL/DL ratios (*i.e.*, applications with very large download volumes, in the left inset) as well as a higher probability of high UL/DL ratios (*i.e.*, services with substantial uploads, in the right inset). For the latter behavior, it is worth noting that a single application has a UL/DL ratio higher than one in 4G, whereas around 7% of services break that barrier in 5G, and generate more traffic in uplink than in downlink.

To further investigate this phenomenon, we compute the percent change of UL/DL ratio between 4G and 5G. Formally, let us denote by ρ^s_{4G} and ρ^s_{5G} the UL/DL ratios for service s in 4G and 5G, respectively; then the percent change of s is

$$C^s = \begin{cases} 100\left((\rho^s_{5G}/\rho^s_{4G}) - 1\right) & \text{if } \rho^s_{5G} \geq \rho^s_{4G} \\ -100\left((\rho^s_{4G}/\rho^s_{5G}) - 1\right) & \text{otherwise.} \end{cases} \quad (2)$$

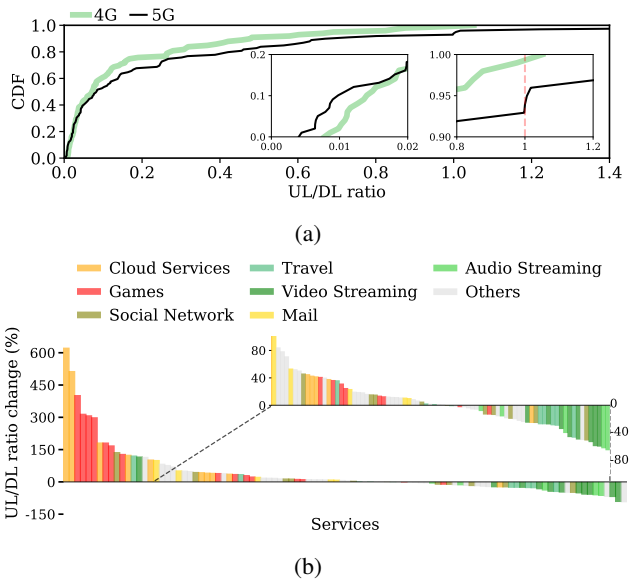

Fig. 6: (a) CDF of UL/DL ratio across services in 4G and 5G. (b) Percent change in the UL/DL ratio from 4G to 5G.

Here, positive values of C^s correspond to the percent growth of uplink traffic prevalence induced by 5G for service s, whereas negative values denote a percent growth of downlink prevalence with 5G. For instance, C^s=60% means that the fraction of traffic of s due to uploads grows by 60% in 5G with respect to $4G$ (with a consequent reduction of relative importance of downlink traffic); conversely, C^s=−30% signifies that downloads expand their weight on the overall traffic of s by 30% when users upgrade from 4G to 5G. C^s is 0% if the UL/DL ratio does not vary across technologies.

Figure 6b shows the results for the top 100 services ranked by C^s, and uncovers that the differences between 4G and 5G CDFs in Figure 6a are due to changes in individual services. Indeed, Figure 6b proves how some applications experience an increased incidence of uplink traffic with 5G (with positive percent changes, on the left of the plot), while others see increased quantities of downloads with 5G (with negative percent changes, on the right). The magnitude of these changes is in fact impressive for many services, with absolute (positive or negative) changes above 50% for 25 applications (*i.e.*, one fourth of the total), proving that the transition to 5G has a major impact on the way users consume many services. In some cases, the effect is dramatic, with changes above 100%, hence more than doubled incidence of uploads or downloads.

Labeling applications by their class (*i.e.*, color) reveals a neat pattern where gaming, Cloud and mail constitute the bulk of services with increased uplink traffic prevalence, whereas video and audio streaming dominate applications with a relative growth of downloads in 5G. It is immediate to correlate these dynamics with the inherent usage of the services:

- the first group above gathers applications that are uplink-oriented, where the availability of high-performance 5G connectivity may invite users to, *e.g.*, rely on the cellular network for Cloud uploads of large files that they would not transfer via 4G, or to enjoy optimized gaming experience via more frequent client-side updates emitted;
- the second group brings together applications that are clearly downlink-intensive, whose users may exploit the capacity of 5G to, *e.g.*, watch higher quality streams, scroll faster through a larger number of video posts, or simply endure longer sessions with each service.

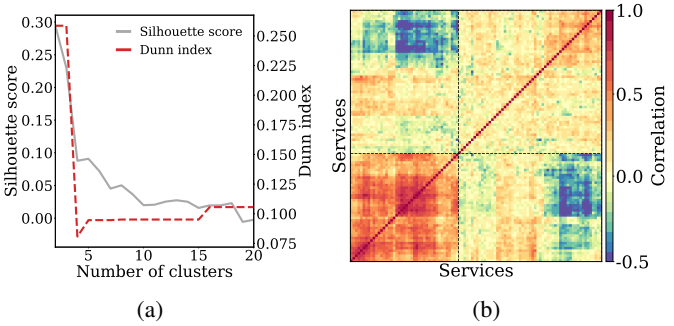

Fig. 7: (a) Silhouette score and Dunn index computed on the hierarchical clustering of service-level 5G ratio median weeks. (b) Correlation matrix of clustered mobile applications.

In both cases, the result points to a magnified usage of many services, whose uplink or downlink nature is dilated by 5G.

Key insights. *Access to 5G noticeably affects the way users consume mobile applications. The improved capacity pushes subscribers to intensify their use of many services, seemingly closing the gap with high-speed fixed Internet usages.*

VI. Mobile Services and Spatiotemporal 5G Usage

In Section IV, we revealed a significant diversity of 5G adoption across time, *i.e.*, over the week, and space, *i.e.*, within each urban area. The explanations to such heterogeneity are deeply rooted in the spatiotemporal fluctuations of 5G demands of individual services, which we investigate next.

A. How do services contribute to 5G time dynamics?

Along the time dimension, we aim at understanding how the temporal dynamics of individual services contribute to the periodic pattern of overall 5G incidence observed in Figure 3. To this end, we compute the median week of 5G ratio of each service s as the hourly median of $R^s_{5G}(t) = 1/L \cdot \sum_\ell R^{\ell,s}_{5G}(t)$, where $R^{\ell,s}_{5G}(t)$ is the fraction of demand for application s that is served by 5G at ℓ during t. We then cluster the service-level median weeks so as to identify recurring behaviors. Specifically, we use the correlation distance, which naturally avoids scale effects and focuses on the likeness of time fluctuations, to compute the pairwise similarity of $R^s_{5G}(t)$ median weeks between any two applications. An agglomerative hierarchical clustering is run on the pairwise distances to build a dendrogram of services. We use the Silhouette score and Dunn index to determine the optimal cut of the dendrogram and number of clusters: as shown in Figure 7a, both metrics present their main drops after a value 2 and no further relevant changes, hence pinpointing the existence of two main behaviors only. The correlation matrix, in Figure 7b, details how applications in Cluster A (bottom left) show a

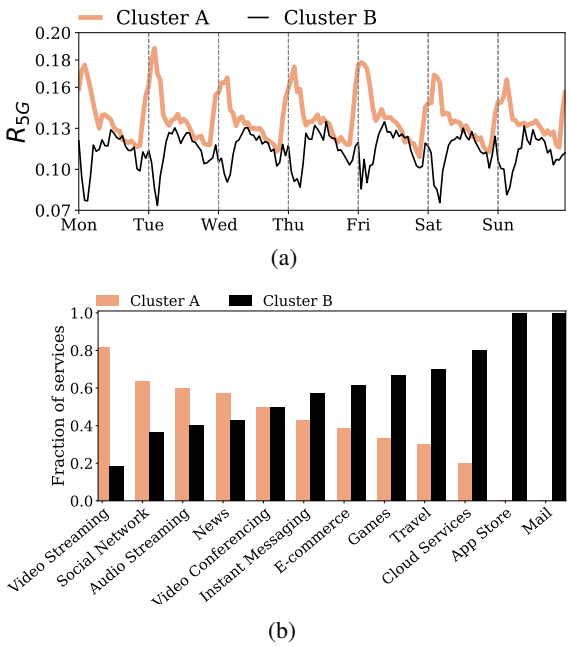

Fig. 8: (a) Average $R^s_{5G}(t)$ median weeks, and (b) breakdown of composition across service classes, for Clusters A and B.

very strong similarity among themselves with high correlations above 0.5. Instead, services in the Cluster B (top right) have weaker mutual resemblance, and are mostly characterized by the fact that they have a high distance from the Cluster A.

To interpret the two behaviors, we portray in Figure 8a the average median weeks of 5G ratio computed over all services in each cluster. Two remarks are in order:

- during the active hours (7:00–22:00), the dynamics of the two clusters do not show significant differences, and they both align to the behavior already observed in Figure 3a of a decreasing incidence of 5G traffic in the afternoon;
- patterns instead diverge in the evening and overnight, where services in Cluster A exhibit the high 5G ratio peak that is also characterizing the overall traffic in Figure 3a, whereas applications in Cluster B show a much smaller peak from 22:00 to midnight followed by a noticeable extra drop in the contribution of 5G to the total traffic.

We further characterize the clusters by analysing the specific applications they bring together. Figure 8b shows the fraction of service classes that are associated to Cluster A or B. Video streaming and social media are strongly characterized by the 5G ratio pattern with high overnight incidence, whereas mail, Cloud and gaming do not show that night peak.

By combining these results, we make the following observations on the causes of the overall temporal behavior observed in Section IV-B. First, the fluctuations in Figure 3a during the active hours are orthogonal of the type of mobile application, as the two predominant service-driven time patterns in Figure 8a both present the same dynamic of a higher 5G incidence in the morning that progressively diminishes in the afternoon. Second, the peak during the evening and overnight period in Figure 3a can be conversely ascribed to a specific

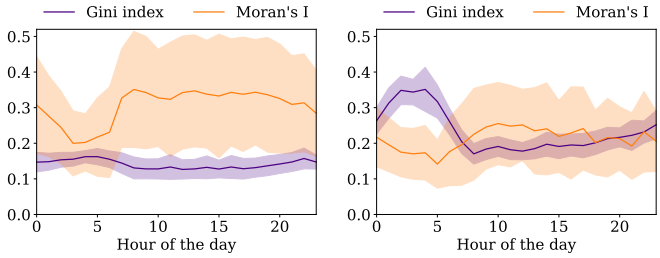

Fig. 9: Gini index and Moran's I of zone-level R_{5G} in time.

subset of mobile services; by looking at the overlap of service classes in Cluster A and in the right part of Figure 6b, those are download-intensive applications that generate the highest demands in the network at all times, and therefore hide the patterns of other applications in the traffic aggregate.

Key insights. *The contribution of 5G traffic to the load generated by individual services follows comparable dynamics across all applications during daylight hours. Overnight, services are instead split between download-oriented ones that see a surge of 5G contribution to the total traffic, and others, including work-oriented applications, that do not experience the relative night peak in 5G demands.*

B. Is there a spatial component to service-level 5G usage?

We are interested in understanding if the diverse service-level time behaviors identified in the previous section have a geographical component, *i.e.*, are affected by specific areas of an urban region. This analysis is also motivated by a previous observation, in Section IV-C, that individual cities see substantial heterogeneity in the 5G incidence R_{5G} across their internal statistical zones.

We start by computing high-level spatial statistics for the time-varying maps of the 5G ratio at the level of individual statistical zones, drawn from the overall traffic generated by Cluster A and Cluster B, respectively. Specifically, Figure 9 shows the Gini index, which measures inequality in the values of $R^\ell_{5G}(t)$ across zones ℓ of a same city during a same time t, and Moran's I, which instead quantifies the spatial correlation among nearby zones at a given time. The two plots highlight striking differences in the spatial properties of Clusters A and B: the former in particular yields a more regular spatial structure of the 5G incidence that is both more homogeneous (*i.e.*, lower Gini index) and smoother (*i.e.*, higher Moran's I) at all times; the latter is more diverse and noisy in space.

Given that Cluster A is predominant in terms of overall traffic, more interesting from a temporal perspective due to its contribution to the nighttime peaks, and also more structured over space, we focus our analysis on that cluster hereinafter.

We thus compute the median week of the 5G ratio at each zone ℓ of the 15 major cities in France, for services that fall in Custer A only. Formally, let us denote by $\mathcal{S}_A$ the set of services in Cluster A, according to the clustering from Section VI-A. Then we compute the 5G ratio for the whole cluster A at each location ℓ and time step t, which we indicate by $R^{\ell,\mathcal{S}_A}_{5G}(t)$, by

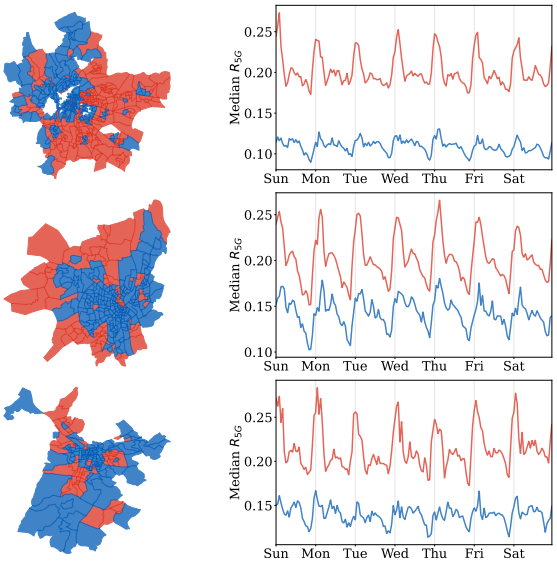

Fig. 10: Maps of the blue and red clusters obtained from the clustering of $R_{5G}^{\ell,\mathcal{S}_A}(t)$ across city locations (left), and corresponding average median weeks (right), for three sample urban areas among the 15 considered in our analysis.

using expression (1) on the total 4G and 5G traffic generated by all applications in $\mathcal{S}_A$. Finally, we calculate the hourly median of such values at each location ℓ during a week.

Within each city, we then cluster these median weeks across locations ℓ, using a similar technique as that employed in Section VI-A. As in that case, we employ an agglomerative hierarchical clustering algorithm on pairwise distances between the median weeks of $R_{5G}^{\ell,\mathcal{S}_A}(t)$ for all locations ℓ of a same city. The only difference is that now we employ an Euclidean distance, as in this case we are also interested in the scale (and not only quality) of the phenomenon across urban areas. Finally, we use again the Silhouette score and Dunn index to determine the best clustering in the resulting dendrogram.

In all cities, the stopping rules above always return two clusters. By juxtaposing results across cities, we observe that in fact the two clusters always have the same distinguishing properties, hence we denote them as 'blue' and 'red' in the following. Figure 10 shows an example for three cities from our set of 5. On the right, we can observe the average median weeks of $R_{5G}^{\ell,\mathcal{S}_A}(t)$ for the two blue and red clusters, which gather statistical zones that are characterized as follows:

- in the blue cluster, we have zones with low 5G adoption for the services in Cluster A that we are studying; moreover, and quite surprisingly, these zones do not show the typical nighttime peaks in the 5G ratio that were the distinctive feature of Cluster A in the the temporal analysis as seen in Figure 8a;
- zones in the red cluster show instead a significantly higher 5G incidence for Cluster A applications, and are indeed marked by the typical strong overnight peak in $R_{5G}^{\ell,\mathcal{S}_A}(t)$.

The same figure shows on the left the maps of the considered sample cities, with statistical zones colored according to the spatial (blue or red) cluster they are associated with. It is easy

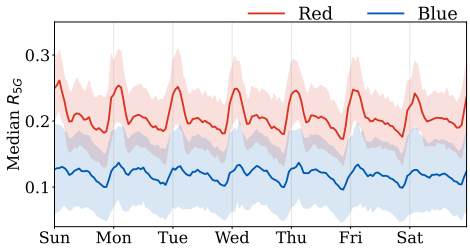

Fig. 11: Average median weeks (with standard deviation) of $R_{5G}^{\ell,\mathcal{S}_A}(t)$ across all cities, for the blue and red clusters.

to spot the emergence of spatial patterns that split cities into groups of adjacent neighborhoods with the same behavior,

A more quantitative result is shown in Figure 11, which summarizes the time series of the $R_{5G}^{\ell,\mathcal{S}_A}(t)$ median weeks for both blue and red clusters observed across all cities in the dataset. The shapes are consistent with the qualitative analysis on the three samples in Figure 10, as we see a rather clear pattern in the red cluster of (i) higher 5G penetration and (ii) nighttime peaks in the incidence of 5G on total traffic.

Based on these results, several considerations are in order:

- first, these clustering results let us postulate that the high values of the 5G contribution to the total traffic that are observed overnight for download-intensive mobile services are in fact a highly localized phenomenon that only characterizes specific areas of each city;
- second, the diurnal fluctuations in the 5G adoption, showing a decreasing trend throughout the afternoon are once more present across both clusters, which points again to a temporal trend that affects the 5G technology as a whole;
- third the high heterogeneity in R_{5G}^{ℓ} recorded within individual cities in Section IV-C can be attributed to a dichotomy of neighborhoods in urban areas, which are separated into regions of high and low 5G penetration.

Key insights. *While the daylight incidence of 5G demands on the total mobile traffic is uniform over space and time, the characterizing high incidence of 5G activity overnight is in the end due to the way a subset of major downlink-oriented services are consumed in specific neighborhoods of cities. The diurnal trend of a relative reduction of 5G traffic with respect to 4G during the afternoon seems to instead affect all services and all urban regions in the exact same way.*

C. Which factors explain the observed 5G adoption?

As a final step in our study, and in order to close the loop in the observed spatiotemporal dynamics of 5G adoption, we aim at providing explanations about the root causes behind the results in Section VI-A and Section VI-B.

To this end, we collect a number of features about the socioeconomic status (SES) and land use that characterize each statistical zone in the 15 cities in our dataset. Specifically, we look at SES metrics that capture the educational level (*e.g.*, fraction of the local population with a university degree), economic status, (*e.g.*, deciles of the distribution of income by the local population), employment status (*e.g.*, fraction of the local population with executive or intellectual professions),

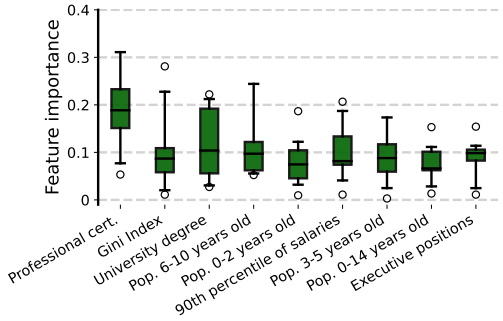

Fig. 12: Importance of the main features used by the RF classifier of the statistical zones across blue and red clusters.

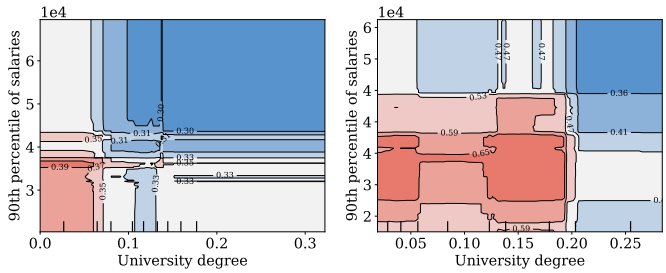

Fig. 13: Partial dependence plots for two sample cities, showing the marginal contribution of the 90^{th} percentile of the income and the percentage of the adult population holding a university degree on the classification.

and population status (*e.g.*, fraction of the local population within multiple given age ranges). We also consider land use statistics, such as the fraction of the surface of each statistical zone that is covered by, *e.g.*, residential or commercial buildings, industrial infrastructures, religious or sports facilities.

We then train a Random Forest (RF) on such feature, with the aim of predicting whether a statistical zone belongs to the blue or red cluster based on SES and land use information. The RF consists of 100 decision trees, each with a maximum node density of 100. We use the Gini index to partition the nodes during construction, where each tree can consider 8 features at the time of partitioning. In addition, to avoid overfitting, we impose the condition that at least 10 samples must be considered for partitioning and that each leaf node must contain at least 3 samples.

Overall, we find that the provided features allow the RF model to determine with a mean 0.79 F1 score, *i.e.*, a fairly high accuracy, the class of the statistical zone. In fact, when looking at feature importance, in Figure 12, we note that land use features are given a negligible weight and essentially not used for classification. Therefore, we conclude that SES is what primarily drives the temporal pattern in 5G adoption across the urban regions, and in particular allows explaining where we can expect the surge of 5G incidence overnight that characterizes the statistical zones in the red cluster.

Figure 13 shows additional information that helps understanding how the RF operates. The figure presents two partial dependence plots obtained from the RF classifier for two sample urban areas. A two-way partial dependence curve is shown as a contour plot, highlighting the marginal contribution of two main selected features on the zone classification: (i) the 90^{th} percentile of salaries, and (ii) the percentage of the adult population holding a university degree. These plots are useful to observe the overall trends of the selected features by marginalizing all other features used in the RF model. In particular, they reveal that, on an aggregate level, the RF model tends to consistently classify low-income and less-educated zones as red, *i.e.*, to match them with the statistical zones marked by the typical nighttime peaks in the 5G ratio. While the figure is a qualitative sample, we find the correlation with social status above to be consistent for the other features.

Our hypothesis is that inhabitants of neighborhoods that are less affluent are nowadays taking advantage of the availability of 5G 'dongles', *i.e.*, small modems that allow creating a Wi-Fi network exploiting the 5G cellular connectivity, to get high-speed Internet access at home at a much lower cost than with regular fiber. This would explain the overnight peaks, due to, *e.g.*, high-quality streaming or automated large file download activities that may characterize home usages during the evening and later into the night. While speculative, this account would be consistent with other effects, *e.g.*, the fact that those same less rich areas record a higher incidence of 5G traffic at all times (see Figure 8a), or that services use intensifies in a home-like way with 5G (see Figure 6b).

Key insights. *Significant explainability with socioeconomic status indicators points at that overnight peaks, as well as other phenomena observed throughout our study, are determined by a significant consumption of 5G as a proxy for home access in less affluent urban areas in France.*

VII. Conclusions

We carried out a first-of-its-kind analysis of 5G adoption and its impact on service consumption, using large-scale measurement collected in an operational nationwide mobile network. Our study takes an original network- and service-oriented perspective on the utilization of the 5G technology, which sets it apart from previous works that looked into 5G performance, mainly from the end user viewpoint. As such, our approach lets us unveil a number of interesting and partially unexpected patterns in the incidence of 5G demands. The main limitation of our study is that it focuses on one mobile network operator and a specific country: hence, we do not pretend that the results generalize globally, but we expect that they may hold, *e.g.*, for a substantial portion of Europe.

Acknowledgment

This work was supported by NetSense, grants no. 2019-T1/TIC-16037 and 2023-5A/TIC-28944, funded by Comunidad de Madrid; by CoCo5G, grant no. ANR-22-CE25-0016, funded by the French National Research Agency; by BANYAN, grant no. 860239, funded by European Union's Horizon 2020 program; and by AEON-ZERO, project no.TSI-063000-2021-52, funded by Spanish Ministry of Economic Affairs and Digital Transformation and the European Union-NextGenerationEU.

REFERENCES

[1] Ericsson, "Ericsson Mobility Report," Jun 2023.

[2] A. Narayanan, X. Zhang, R. Zhu, A. Hassan, S. Jin, X. Zhu, X. Zhang, D. Rybkin, Z. Yang, Z. M. Mao, *et al.*, "A variegated look at 5g in the wild: performance, power, and qoe implications," in *Proceedings of the 2021 ACM SIGCOMM 2021 Conference*, pp. 610–625, 2021.

[3] A. Narayanan, M. I. Rochman, A. Hassan, B. S. Firmansyah, V. Sathya, M. Ghosh, F. Qian, and Z.-L. Zhang, "A comparative measurement study of commercial 5g mmwave deployments," in *IEEE INFOCOM 2022-IEEE Conference on Computer Communications*, pp. 800–809, IEEE, 2022.

[4] A. Narayanan, E. Ramadan, J. Carpenter, Q. Liu, Y. Liu, F. Qian, and Z.-L. Zhang, "A first look at commercial 5g performance on smartphones," in *Proceedings of The Web Conference 2020*, pp. 894–905, 2020.

[5] Y. Liu and C. Peng, "A close look at 5g in the wild: Unrealized potentials and implications," in *IEEE INFOCOM 2023-IEEE Conference on Computer Communications*, IEEE, 2023.

[6] C. Fiandrino, D. Juárez Martínez-Villanueva, and J. Widmer, "Uncovering 5g performance on public transit systems with an app-based measurement study," in *Proceedings of the 25th International ACM Conference on Modeling Analysis and Simulation of Wireless and Mobile Systems*, pp. 65–73, 2022.

[7] Y. Pan, R. Li, and C. Xu, "The first 5g-lte comparative study in extreme mobility," *Proceedings of the ACM on Measurement and Analysis of Computing Systems*, vol. 6, no. 1, pp. 1–22, 2022.

[8] D. Xu, A. Zhou, X. Zhang, G. Wang, X. Liu, C. An, Y. Shi, L. Liu, and H. Ma, "Understanding operational 5g: A first measurement study on its coverage, performance and energy consumption," in *Proceedings of the Annual conference of the ACM Special Interest Group on Data Communication on the applications, technologies, architectures, and protocols for computer communication*, pp. 479–494, 2020.

[9] X. Yang, H. Lin, Z. Li, F. Qian, X. Li, Z. He, X. Wu, X. Wang, Y. Liu, Z. Liao, *et al.*, "Mobile access bandwidth in practice: Measurement, analysis, and implications," in *Proceedings of the ACM SIGCOMM 2022 Conference*, pp. 114–128, 2022.

[10] P. Parastar, A. Lutu, G. Alay, Ozguand Caso, and D. Perino, "Spotlight on 5g: Performance, device evolution and challenges from a mobile operator perspective," in *IEEE INFOCOM 2023-IEEE Conference on Computer Communications*, IEEE, 2023.

[11] P. Fiadino, M. Schiavone, and P. Casas, "Vivisecting whatsapp through large-scale measurements in mobile networks," in *Proceedings of the 2014 ACM Conference on SIGCOMM*, SIGCOMM '14, (New York, NY, USA), p. 133–134, Association for Computing Machinery, 2014.

[12] Q. Deng, Z. Li, Q. Wu, C. Xu, and G. Xie, "An empirical study of the wechat mobile instant messaging service," in *2017 IEEE Conference on Computer Communications Workshops (INFOCOM WKSHPS)*, pp. 390–395, 2017.

[13] J. Erman, A. Gerber, K. K. Ramadrishnan, S. Sen, and O. Spatscheck, "Over the top video: The gorilla in cellular networks," in *Proceedings of the 2011 ACM SIGCOMM Conference on Internet Measurement Conference*, IMC '11, (New York, NY, USA), p. 127–136, Association for Computing Machinery, 2011.

[14] Z. Li, X. Wang, N. Huang, M. A. Kaafar, Z. Li, J. Zhou, G. Xie, and P. Steenkiste, "An empirical analysis of a large-scale mobile cloud storage service," in *Proceedings of the 2016 Internet Measurement Conference*, IMC '16, (New York, NY, USA), p. 287–301, Association for Computing Machinery, 2016.

[15] Y. Zhang and A. Årvidsson, "Understanding the characteristics of cellular data traffic," *SIGCOMM Comput. Commun. Rev.*, vol. 42, p. 461–466, sep 2012.

[16] C. Marquez, M. Gramaglia, M. Fiore, A. Banchs, C. Ziemlicki, and Z. Smoreda, "Not all apps are created equal: Analysis of spatiotemporal heterogeneity in nationwide mobile service usage," in *Proceedings of the 13th International Conference on Emerging Networking EXperiments and Technologies*, CoNEXT '17, (New York, NY, USA), p. 180–186, Association for Computing Machinery, 2017.

[17] A. Okic, A. E. Redondi, I. Galimberti, F. Foglia, and L. Venturini, "Analyzing different mobile applications in time and space: a city-wide scenario," in *2019 IEEE Wireless Communications and Networking Conference (WCNC)*, pp. 1–6, 2019.

[18] I. Trestian, S. Ranjan, A. Kuzmanovic, and A. Nucci, "Measuring serendipity: Connecting people, locations and interests in a mobile 3g network," in *Proceedings of the 9th ACM SIGCOMM Conference on Internet Measurement*, IMC '09, (New York, NY, USA), p. 267–279, Association for Computing Machinery, 2009.

[19] Q. Xu, J. Erman, A. Gerber, Z. Mao, J. Pang, and S. Venkataraman, "Identifying diverse usage behaviors of smartphone apps," in *Proceedings of the 2011 ACM SIGCOMM Conference on Internet Measurement Conference*, IMC '11, (New York, NY, USA), p. 329–344, Association for Computing Machinery, 2011.

[20] M. Z. Shafiq, L. Ji, A. X. Liu, J. Pang, and J. Wang, "Characterizing geospatial dynamics of application usage in a 3g cellular data network," in *2012 Proceedings IEEE INFOCOM*, pp. 1341–1349, 2012.

[21] M. Z. Shafiq, L. Ji, A. X. Liu, and J. Wang, "Characterizing and modeling internet traffic dynamics of cellular devices," *SIGMETRICS Perform. Eval. Rev.*, vol. 39, p. 265–276, jun 2011.

[22] R. Keralapura, A. Nucci, Z.-L. Zhang, and L. Gao, "Profiling users in a 3g network using hourglass co-clustering," in *Proceedings of the Sixteenth Annual International Conference on Mobile Computing and Networking*, MobiCom '10, (New York, NY, USA), p. 341–352, Association for Computing Machinery, 2010.

[23] H. Li, X. Lu, X. Liu, T. Xie, K. Bian, F. X. Lin, Q. Mei, and F. Feng, "Characterizing smartphone usage patterns from millions of android users," in *Proceedings of the 2015 Internet Measurement Conference*, IMC '15, (New York, NY, USA), p. 459–472, Association for Computing Machinery, 2015.

[24] F. Aurenhammer, "Voronoi diagrams—a survey of a fundamental geometric data structure," *ACM Comput. Surv.*, vol. 23, sep 1991.

[25] European Union, "Eu general data protection regulation (gdpr): Regulation (eu) 2016/679 of the european parliament and of the council of 27 april 2016 on the protection of natural persons with regard to the processing of personal data and on the free movement of such data, and repealing directive 95/46/ec (general data protection regulation)," Jun 2016.

[26] M. Z. Shafiq, L. Ji, A. X. Liu, and J. Wang, "Characterizing and modeling internet traffic dynamics of cellular devices," in *Proceedings of the ACM SIGMETRICS Joint International Conference on Measurement and Modeling of Computer Systems*, SIGMETRICS '11, (New York, NY, USA), p. 305–316, Association for Computing Machinery, 2011.

[27] C. K. Kim and S. Ian, *Examining Applied Multicultural Industrial and Organizational Psychology*, ch. Why Do People Still Buy Apple Products?: Applying Psychological Modeling to Brand Image Management and Cultural Business Ecosystems. IGI Global, 2023.